Notch Sensitivity and Fracture Resistance of Non-woven Felts

A. Ridruejo[1], C. González[1,2], J. LLorca[1,2]
[1]*Universidad Politécnica de Madrid, Madrid, Spain;*
[2]*IMDEA-Materiales, Madrid, Spain*

Abstract

Non-woven felts are made of networks of individual fibers or fiber bundles deposited over a planar surface. Bonds between fibers are introduced by means of mechanical needles, thermal fusion or chemical bonds to increase the stiffness and strength of nonwovens. An experimental and computational study of the notch sensitivity of a glass fiber non-woven felt is presented here. To this end, tensile tests were carried out on unnotched and notched specimens. The dominant failure mechanism was fiber-fiber bond rupture and damage was localized in a narrow zone close to the notch tip, whose size was limited by the fiber length. The fracture behavior was simulated using the finite element method with Abaqus Explicit. Fibers were modeled using standard beam elements and bonds between fibers were taken into account using connector elements. The numerical predictions of the notch sensitivity were compared with experimental results and showed the potential of computational mechanics to accurately reproduce the damage pattern and the failure strength.

1. Introduction.

Nonwoven felts are materials manufactured from a set of disordered fibres consolidated by bonds of different nature, such as simple entanglement, local thermal fusion or chemical binders, depending on the particular material or processing technique. Their mechanical properties are good in terms of ultimate strength, albeit generally lower than their woven counterparts. On the other hand, they show both outstanding deformation capability and unmatched energy absorption during the deformation process.

Nowadays, their range of applications has been extended to fields such as ballistic protection, isolating materials, liquid-absorbing textiles, fireproof layers, or geotextiles for soil reinforcement [1]. Paper is a particularly significant example of a nonwoven felt, with cellulose fibers linked by hydrogen bonds [3,4]. Recently, further research in this field has been stimulated as a consequence of its structural analogy with biological tissues and the advent of fibers with reduced manipulability, with carbon nanotubes as a paradigmatic example [2].

The mechanical behavior of nonwoven felts is highly complex, because it simultaneously involves deformation and fracture phenomena such as large

deformations, bond breakage as well as rotations, sliding and fracture of fibers. Whereas analytical numerical models greatly improve our understanding of the mechanical behavior of nonwoven felts [5-12], they sometimes may rely upon *ad hoc* assumptions and adjusting parameter values which are not always well determined. The relative lack of scientific references on the field and the fact that most of the available information [14] comes from the market-oriented manufacturers are two of the present main obstacles.

This justifies the interest in obtaining a deeper knowledge of the mechanical properties of nonwovens, both from an experimental and computational point of view, taking into account not only the microstructure, but also the previously mentioned mechanisms of deformation and fracture. This paper shows experimental results from fracture tests performed on a commercially available felt made of glass fibers and the comparison with a computational model of these tests.

2. Material

The fiber glass nonwoven felt under study was the Vetrotex M123, manufactured by Saint Gobain Vetrotex [18] and widely used as a reinforcing material for many structural applications, particularly those which require a reliable behavior when exposed to aggressive chemical agents. Figures (1) and (2) show its microstructure.

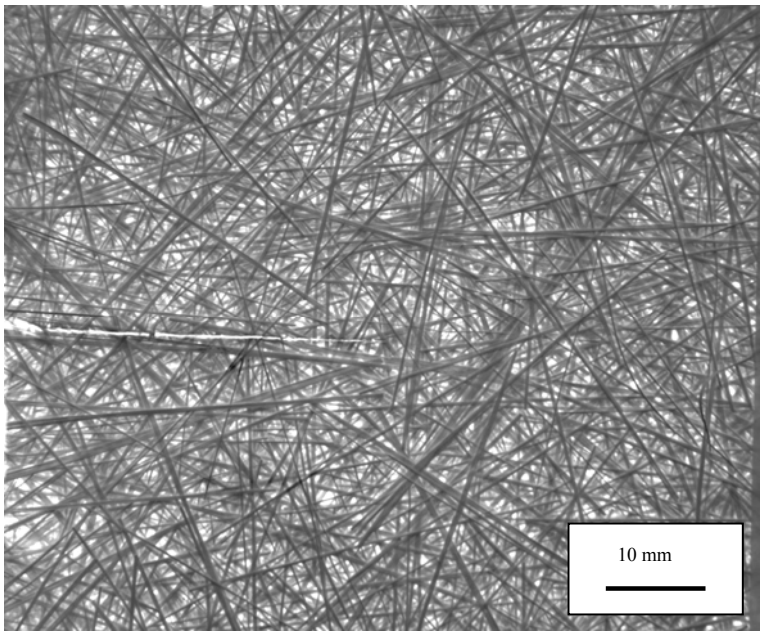

Figure 1. *Vetrotex M123 Chop Strand Mat*

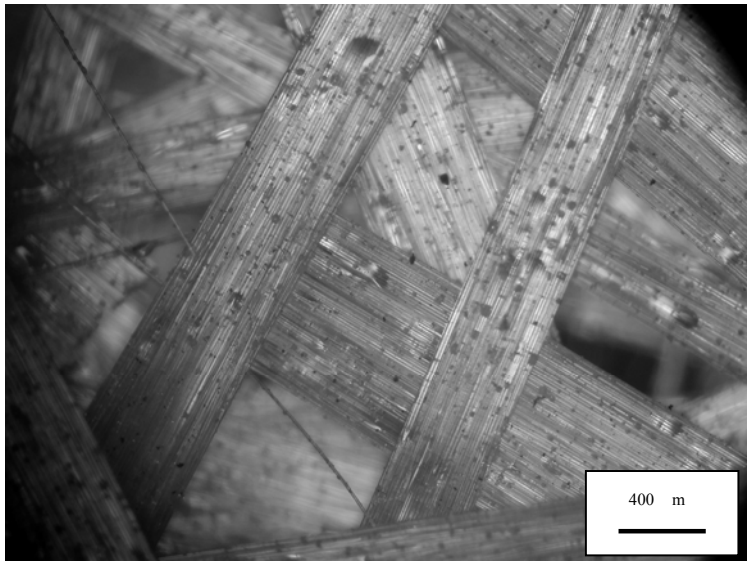

Figure 2. Vetrotex M123 Chop Strand Mat. Detailed view of the fiber bundles.

The felt is composed of 10-micron diameter E-type glass fibers bound together forming bundles of 50 mm of length with an approximate rectangular cross section of 560 μm x 50 μm. The fibers are covered with an organic powder binder in order to improve its possible later impregnation with a resin. This binder endows the felt with a certain initial consistency. While it is not apparent, the nonwoven felt possesses a multilayer structure. The total thickness is equivalent to five times the thickness of a fiber bundle.

3. Experimental techniques

The goal of this work is to systematically study the mechanical behavior of the nonwoven felts described in the previous section. Samples of 200 mm x150 mm were cut along the roll direction in order to perform uniaxial tensile tests complying with the EN ISO 10319 standard requirements. The felt density was obtained from direct mass measurements (AND HF 1200G analytical balance) and the dimensions of the specimens. The results showed an average density of 454 6 g/m^2. Tests were carried out in an electromechanical testing machine (Instron 1122) under stroke control at a cross head speed of 0.2 mm/s
The applied load was measured with a 5kN load cell.
The notch sensitivity was studied by cutting a central notch whose length was equal to 20 %, 40 % or 60 % of the sample width. All the notches were introduced by cutting the fiber bundles with a standard steel blade.

The felt microstructure was observed by means of a profile projector (Nikon V12B), and a conventional optical microscope (Nikon Metaphot). This microscope allowed the acquisition and subsequent processing of images. Polarized light and sample dyeing enhanced the image contrast to a great extent. The fiber orientation showed an isotropic distribution in all cases.

3.1 Tensile tests on unnotched specimens

The mechanical behavior of the non-woven felts was characterized from its nominal stress-strain curve, which led to three main measurements. First, the stiffness was obtained as a secant modulus corresponding to 1% of strain. Secondly, the strength was computed as the maximum load during the test per unit width. Finally, the specific absorbed energy was calculated as the area under the force-displacement curve divided by the planar area of the specimen (table 1)

Material	E_s , 1% (kN/m)	Strength (kN/m)	W_{abs} (J/m^2)
Vetrotex M123	40 ± 8	3.0 ± 0.8	50± 8

Table 1. Mechanical properties of the Vetrotex M123 mat

Figure (3) shows a characteristic plot of stress (force per unit width) versus nominal strain for a fiberglass non-woven felt. Load increases linearly until it reaches a maximum with the shape of a sharp peak. This maximum corresponds to the damage localization (nominal strain around 1%) due to loss of adhesion between fiber bundles. From this precise moment on, the fiber bundles in the damaged area start to slide, and therefore the residual strength is a consequence of the friction among fibers. For a strain in the range of 20-25%, the material loses practically all its load carrying capability.

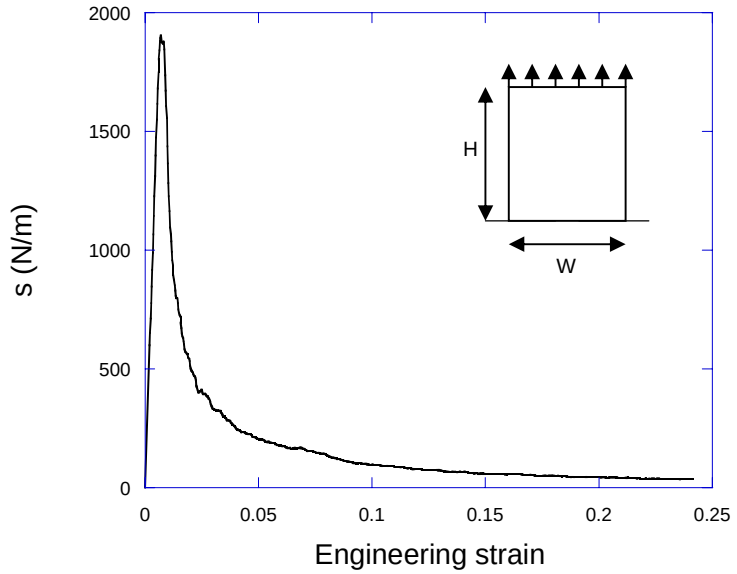

Figure 3. Characteristic stress-strain curve of a tensile test, Vetrotex M123 mat

3.2 Notched tensile tests

The fracture behavior of the non-woven felts was studied by using the same uniaxial tensile test samples, now endowed with a central notch of increasing length equal to the 0.2, 0.4 and 0.6 fractions of the total specimen width.
The mechanical strength of the notched specimens adimensionalized by the tensile strength of the felt is shown in figure 4 as a function of the relative notch size. The mechanical strength of a fracture sample made of a notch-insensitive material is given by

$$s/s_R = 1-(2a_0/W), \qquad \text{(Equation 1)}$$

where W is the specimen width, $2a_0$ the notch length and s_R the strength of the unnotched material. This law establishes a linear relationship between the residual strength and the size of the notch. As we can observe in figure (4), the residual strength of the felt decreases slightly faster than its prediction by equation (1) and the material shows notch-sensitive behavior in accordance with the brittle one observed in the tensile tests performed on the unnotched specimens.

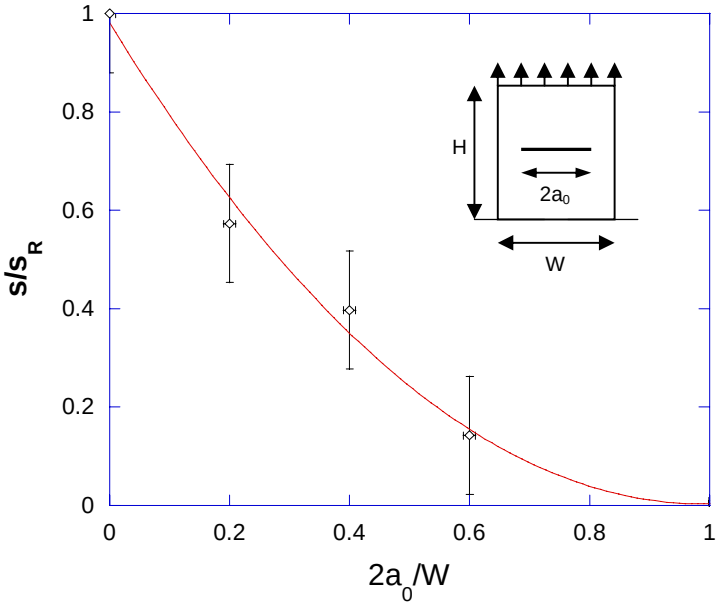

Figure 4. Strength versus relative notch size. Vetrotex M123 mat

From the viewpoint of structural damage, the fibers are not broken in this material. As the fiber bundles are much stronger than their bonds, there is only one damaging mechanism: bond fracture followed by fiber sliding. The relatively short length and stiffness of the fiber bundles limits the spread of damage and consequently, when deformation is localized, the fiberglass felt is bound to break in this zone.

4.Simulations

4.1 Model description

Regarding the internal structure of the felt, we have simulated a representative monolayer based on direct measurements of the free distance between fiber intersections. As the strength increases linearly with the number of layers, the forces arising from the simulations were scaled by a factor equal to the ratio between the actual and the simulated felt densities. The strain measurements are not affected by the internal structure of the felt. The model is based on a 2D random network. A rectangular cell of dimensions H=10 mm and W=20 mm, equal to those used in the experimental tests, is considered. Fibers were deposited individually in a random way. Every single fiber is divided into N segments of the same length, each of them forming an angle α with respect to the previous one. This would allow the model to take into account fibers of arbitrary curvature. The coordinates x_o,y_o for the first segment are randomly generated, and the algorithm continues to place segments until the completion of the total length of the fiber. If a segment falls outside the boundary of the cell, the intersection of the fiber segment with the cell boundary is calculated and the remaining part of the segment is transferred to the opposite boundary of the cell. This method ensures that the actual fiber length placed is equal to the prescribed one.

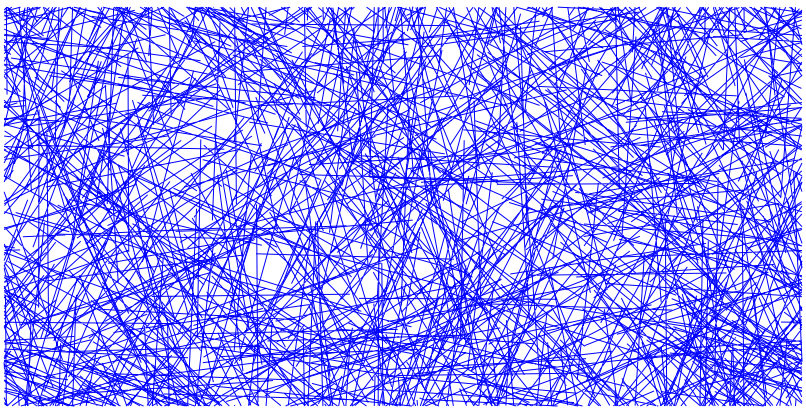

Figure 5. Geometrical model for the fiberglass mat. Undeformed mesh

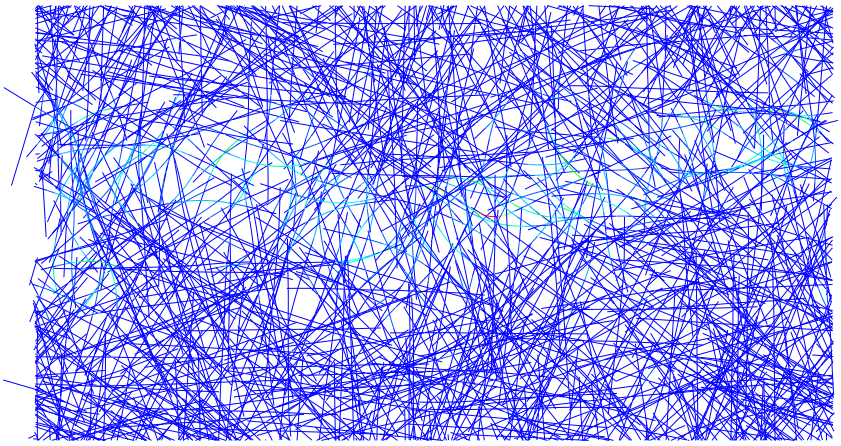

Figure 6. Final state, broken mesh (5x magnification). Note the localized deformation

The fiber network generated using the method described above is discretized with finite elements. Each fiber segment naturally leads to a Timoshenko beam (B31) element with the nodes located at both ends and endowed with the cross sectional geometry of the real fibers.

The model establishes a fiber bond by identifying the two nearest nodes corresponding to different fibers and by linking them with a massless connector element (CONN2D2). For the sake of simplicity, we have used a linear force-displacement law. When the relative displacement of the nodes of the connector reaches a certain value δ_F, assumed to be approximately one half of the bundle width, the force sharply decays to zero and the bond is considered broken. The data for the stiffness and maximum load of the connector elements are those from a standard polystyrene polymeric binder [13]. A model for a full simulation of the deformation and fracture process of this material should include the frictional sliding of the fiber bundles, but this is beyond the scope of this study and it has not been implemented. Once the load reaches its peak and the deformation is localized, the simulations cease to be realistic.

The simulations were carried out with Abaqus Explicit (v. 6.7) under the framework of quasi-static loadings and large displacement theory. In all the simulations the kinetic energy was at least one order of magnitude lower than the strain energy of the model. One of the main advantages of the model is the lack of adjustable parameters, with the threshold displacement δ_F as the only one. The main parameters of the model can be summarized in the following table:

Layer density	Stiffness, fiber bundle	Spring constant, connector	Cross section, bundle	Fiber length	Threshold displacement, δ_F
2.1 mm/mm^2	70 GPa	0.7 N/mm	60x30 μm^2	50 mm	0.25 mm

Table 2. *Model parameters.*

4.2 Results

Figure (7) depicts the experimental representative stress-strain curve and a set of three simulations.

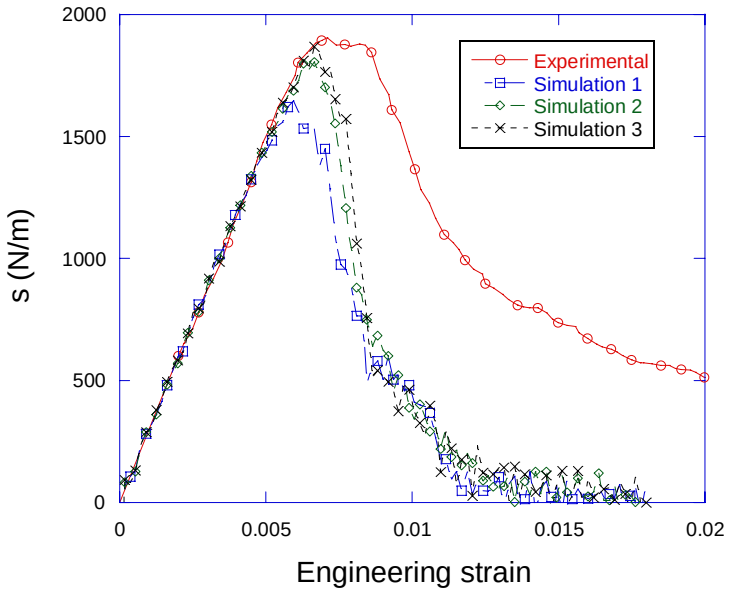

Figure 7. *Numerically-simulated and experimental stress-strain curves*

It can be observed that both the initial stiffness and the maximum stress are in good agreement with the experimental results. The dispersion of the numerical results is relatively small and due to differences in fiber distribution. As can be reasonably expected, the friction between fiber bundles leads to a slower decrease of the load carried by the glass fiber mat which is not matched by the simulations.

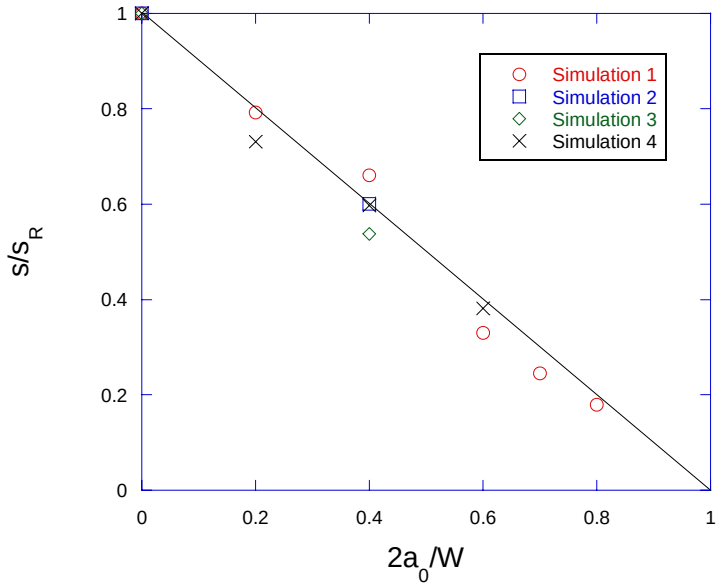

Figure 8. *Strength versus relative notch size. Numerical results.*

Further calculations were carried out in order to ascertain the fracture behavior of notched specimens. Following the experimental method, FEM meshes with centered notches were generated. As can be observed in figure (8), the residual strength of the notched meshes showed a linear decay in accordance with equation (1), therefore not fitting the experimental results.

5.Concluding remarks

Despite its simplicity, the implemented model is able to predict from a relatively reduced amount of experimental data the elastic behavior of a chopped strand mat as well as its damage onset. When the strain is close to 0.7%, the stress reaches its maximum and the felt deformation is localized in a narrow band. From this point on, the damage process is controlled by a frictional mechanism among fiber bundles. This mechanism produces an additional energy dissipation, which prevents the actual felts from undergoing an acute decay of their load-carrying capacity in contrast with the simulations, which lose their strength almost immediately. A new model for taking frictional sliding into account is under consideration.

Regarding the mismatch between the numerical and experimental results for the notched felts, it can be conjectured that the additional damage observed in the experimental results with respect to the linear law expressed in Eq. (1) arise from the tridimensionality of the real felts. Out-of-plane forces would weaken the bonds by acting in mixed fracture modes and not only in a pure shear mode. Nevertheless, this remains as an open question for further research.

Acknowledgements

The authors thank Saint Gobain Vetrotex for its generous supply of the material, the Regional Government of Madrid for the support of this research in the frame of the ESTRUMAT (MAT/0077) program and the Spanish Ministry of Science for its support through the Project MAT2006-2602.

References

[1] Russell, S., ed. (2007), *Handbook of nonwovens*, The Textile Institute, CRC, Woodhead Publishing Ltd.

[2] Berhan, L.; Yi, Y. B.; Sastry, A. M.; Munoz, E.; Selvidge, M. & Baughman, R. (2004), 'Mechanical properties of nanotube sheets: Alterations in joint morphology and achievable moduli in manufacturable materials', *J. Appl. Phys.* **95**(8), 4335--4345.

[3] Cox, H. L. (1952), 'The elasticity and strength of paper and other fibrous materials', *British Journal of Applied Physics* **3**(3), 72--79.

[4] Bronkhorst, C. A. (2003), 'Modelling paper as a two-dimensional elastic-plastic stochastic network', *International Journal of Solids and Structures* **40**(20), 5441--5454.

[5] Åström, J. A.; Krasheninnikov, A. V. & Nordlund, K. (2004), 'Carbon Nanotube Mats and Fibers with Irradiation-Improved Mechanical Characteristics: A Theoretical Model', *Phys. Rev. Lett.* **93**(21), 215503--.
[6] Åström, J. A.; Mäkinen, J. P.; Alava, M. J. & Timonen, J. (2000), 'Elasticity of Poissonian fiber networks', *Phys. Rev. E* **61**(5), 5550--.
[7] Heussinger, C. & Frey, E. (2006), 'Floppy Modes and Nonaffine Deformations in Random Fiber Networks', *Phys. Rev. Lett.* **97**(10), 105501--4.
[8] Hägglund, R. & Isaksson, P. (2008), 'On the coupling between macroscopic material degradation and interfiber bond fracture in an idealized fiber network', *International Journal of Solids and Structures* **45**(3-4), 868--878.
[9] Isaksson, P.; Gradin, P. & Kulachenko, A. (2006), 'The onset and progression of damage in isotropic paper sheets', *International Journal of Solids and Structures* **43**(3-4), 713--726.
[10] Isaksson, P. & Hägglund, R. (2007), 'Evolution of bond fractures in a randomly distributed fiber network', *International Journal of Solids and Structures* **44**(18-19), 6135--6147.
[11] Isaksson, P.; Hägglund, R. & Gradin, P. (2004), 'Continuum damage mechanics applied to paper', *International Journal of Solids and Structures* **41**(16-17), 4731--4755.
[12] S. Heyden, PhD. Thesis. Lund University (2000).
[13] Ramos-Carpio, M. (2007), *Ingenieria de los materiales polimericos*, Fundacion para el fomento de la innovacion industrial
[14] Vetrotex Chopped Strand Mats. Vetrotex Saint Gobain. http://www.vetrotexeurope.com/products/ re_chopstrmat.html (2005)